RESEARCH PAPER

Cell Adhesion & Migration 5:2, 119-132; March/April 2011; © 2011 Landes Bioscience

Formation of microvilli and phosphorylation of ERM family proteins by CD43, a potent inhibitor for cell adhesion

Cell detachment is a potential cue for ERM phosphorylation and organization of cell morphology

Junko Yamane,[1,†] Hiroe Ohnishi,[1,2] Hiroyuki Sasaki,[3] Hisashi Narimatsu,[2] Hajime Ohgushi[1] and Kouichi Tachibana[1,2,*]

[1]Health Research Institute; Tissue Engineering Research Group; National Institute of Advanced Industrial Science and Technology (AIST); Amagasaki, Hyogo Japan; and [2]Research Center for Medical Glycoscience; AIST; Tsukuba, Ibaraki Japan; [3]Department of Molecular Cell Biology; Institute of DNA Medicine; The Jikei University School of Medicine; Minato-ku, Tokyo Japan

[†]Current address: Center for Disease Biology and Integrative Medicine; Graduate School and Faculty of Medicine; The University of Tokyo; Bunkyo-ku, Tokyo, Japan

Key words: cell adhesion, CD43, microvilli, ERM, integrin, cell rounding, phosphorylation, mucin

Abbreviations: BSA, bovine serum albumin; CB, cacodylate buffer; CMO, Cell Mask Orange; DMEM, Dulbecco's modified Eagle's medium; ERM, ezrin/radixin/moesin; FCM, flowcytometry; GA, glutaraldehyde; GST, glutathione S-transferase; OSGEP, *O*-sialoglycoprotein endopeptidase; PB, phosphate buffer; PBS, phosphate-buffered saline; PFA, paraformaldehyde; PLL, poly-L-lysin; TBS, Tris-buffered saline

CD43/sialophorin/leukosialin, a common leukocyte antigen, is known as an inhibitor for cell adhesion. The ectodomain of CD43 is considered as a molecular barrier for cell adhesion, while the cytoplasmic domain has a binding site for Ezrin/Radixin/Moesin (ERM). We found expression of CD43 induced cell rounding, inhibition of cell re-attachment, augmentation of microvilli and phosphorylation of ERM in HEK293T cells. Mutant studies revealed the ectodomain of CD43, but not the intracellular domain, essential and sufficient for all these phenomena. We also found that forced cell detachment by itself induced phosphorylation of ERM in HEK293T cells. Taken together, these findings indicate that inhibition of cell adhesion by the ectodomain of CD43 induces phosphorylation of ERM, microvilli formation and eventual cell rounding. Furthermore, our study suggests a novel possibility that cell detachment itself induces activation of ERM and modification of cell shape.

Introduction

Mounting publications direct activation of Talin and its interaction with integrin as the mechanism for integrin activation.[1-3] Although this can be a long-searched mechanism to activate integrin avidity, there are also other factors that regulate integrin-mediated cell adhesion.

One of such factors is CD43, an inhibitor for various kinds of cell adhesion. CD43 is a cell surface antigen abundantly expressed in various leukocytes.[4,5] Disruption of *cd43* gene in CEM cells resulted in increased β1 integrin-mediated cell adhesion,[6] while T lymphocytes from *cd43*$^{-/-}$ mice showed increase in both β1 and β2 integrin-mediated cell adhesions.[7] Meanwhile CD43 expression in Hela cells inhibited β2 integrin-mediated adhesion with T lymphocytes.[8] Besides integrin-mediated cell adhesion, CD4-mediated cell adhesion to HIV gp120 and L-selectin-mediated tethering were also decreased by CD43.[7,9] PMA-treated thymocytes and bone marrow-derived mast cells from *cd43*$^{-/-}$ mice showed augmented homotypic adhesion compared to those cells from wild-type mice.[7,10] At the same time, CD43 often shows uneven distribution in a cell. In polarized leukocytes, CD43 is localized at the Uropods, the trailing edge of cells.[11,12] Meanwhile, exclusion of CD43 from cell-cell adhesion sites was reported.[13,14] These uneven distribution and exclusion from adhesion sites suggest that the effect of CD43 on cell adhesion is reversible and that CD43 is not a static inhibitor, but a dynamic regulator of cell adhesion.

Then, how does CD43 inhibit cell adhesion? Human CD43 is a type-1 single-pass transmembrane protein of 400 amino acids. CD43, also known as sialophorin or leukosialin, is highly *O*-glycosilated on its ectodomain.[15,16] This throughout

*Correspondence to: Kouichi Tachibana; Email: kouichi-tachibana@aist.go.jp
Submitted: 08/26/10; Revised: 10/08/10; Accepted: 10/11/10
DOI: 10.4161/cam.5.2.13908

O-glycosylation with sialic acids prevents folding of the ectodomain and helps CD43 to protrude from cell surface. The average length of the CD43 ectodomain is 45 nm,[17] which is considered larger than most extracellular domains of cell surface receptors. Based on these structural characteristics, it has been proposed that CD43 protrudes from cell surface and inhibits cell surface receptors to reach their ligands by its height. Although not fully proved, this inhibitory mechanism of CD43 for cell adhesion has been well accepted.

Since CD43 is one of the major *O*-glycosylated proteins in T lymphocytes,[4] we analyzed CD43 as a carrier protein during our investigation of *O*-glycans. We soon experienced various events possibly related to CD43's inhibitiory function for cell adhesion. Furthermore, we found that CD43 expression lead to the formation of microvilli-like protrusions.

Microvilli are cell surface thin protrusions, composed of cytoplasmic membrane and parallel bundles of actin filaments.[18,19] Microvilli are most recognized in epithelial cells of intestinal and renal brush borders and functions of such microvilli include expansion of cell surface area for absorption and molecule presentation and inhibition of cell adhesion.[19] Meanwhile, microvilli are also observed on the surface of lymphocytes and other hematopoietic cells.[20-23] Contradictory roles in cell adhesion were proposed for leukocyte microvilli. Several adhesion receptors are specifically localized on microvilli, and such localization may be critical for the binding to vascular endothelium.[22,24,25] Meanwhile, microvilli in lymphocytes were collapsed by the stimulation of chemokines,[26] suggesting an inhibitory function of microvilli for cell adhesion. Moreover, microvilli of lymphocytes were lost after passing through high endothelial cells,[27] suggesting dynamic regulation of microvilli during extravasation.

Although microvilli and their component proteins have been studied, it is still unclear how microvilli are formed. Recently, several reports indicated the involvement of a few sialomucins in the formation of microvilli. Okumura et al. reported that long form of gicerin/CD146/Muc18/MCAM (melanoma cell adhesion molecule) was localized in microvilli in melanoma cells and induced microvilli elongation in mouse fibroblasts.[28] Guezguez et al. further reported that MCAM augmented the number and extension of microvilli in NKL cells and augmented rolling on endothelial cells.[29] Meanwhile, Nielsen et al. reported that podocalyxin, a CD34-related molecule, was a potent inducer of microvillous formation.[30]

There are several publications suggesting the relations between microvilli and CD43, another sialomucin. Yonemura et al. reported concentration of CD43 at microvilli.[31] Forced expression of a chimeric molecule of E-cadherin ectodomain and CD43 transmembrane/intracellular domain induced elongation of microvilli in mouse fibroblast.[32] This phenomenon has been explained as the effect of recruitment of Ezrin/Radixin/Moesin proteins (ERM) to cellular membrane, since ERM bind juxta-membrane region of CD43's intracellular domain.[33] ERM are observed in various cytoskeleton-based structures including microvilli, and are considered as docking proteins that link cell surface proteins with actin cytoskeleton.[14,19,34-36] Since antisense oligonucleotides to ERM abrogated microvilli,[37] ERM are considered essential for the formation or maintenance of microvilli. However, ERM need conformation changes and activation for the interaction with other proteins.[35,36,38-40] Although the mechanism of ERM activation is not fully revealed yet, phosphorylation on a conserved threonine residue (T567 in Ezrin, T564 in Radixin, T558 in Moesin) are considered as a marker for activated ERM.[32,35,36] Conveniently, ERM that are phosphorylated at this threonine residue can be identifed by anti-phospho-ERM antibodies. Such phosphorylated ERM are observed at microvilli, Uropods and cortex of spherical cells,[26,35,36,41-43] while dephosphorylation of ERM is accompanied with collapse of microvilli by chemokines,[26,41,43] indicating phosphorylated and therefore, activated ERM are essential for the formation and maintenance of these structures. Thus, there should be a mechanism of ERM activation upon formation of microvilli, although it has not been fully revealed yet.

In this article, we demonstrated cell rounding, inhibition of re-attachment, formation of microvilli and phosphorylation of ERM were induced by the expression of CD43 in HEK293T cells. Mutant studies revealed the ectodomain of CD43 essential and sufficient for all these phenomena. Based on further investigation about these phenomena, we propose inhibition of cell adhesion as the mechanism of CD43 to induce ERM phosphorylation, microvilli formation and eventual cell rounding.

Results

CD43 expression induced cell rounding. During investigation for other purposes, we happened to find CD43 expression induced HEK293T cells a switch from a polarized to a spherical shape. To confirm this effect of CD43, we expressed either GFP or CD43-GFP chimeric protein, in which GFP was fused to the C-terminus of CD43, in HEK293T cells and investigated these cells by phase contrast and fluorescent microscopy. In low magnification, we observed most HEK293T cells expressing CD43-GFP were spherical at 40 h after transfection (**Fig. 1Ab and d**), while most GFP-expressing cells were spread (**Fig. 1Aa and c**). Cell surface expression of CD43 was confirmed in CD43-HEK293T cells by flowcytometry (FCM), while endogenous CD43 was not detected in parental HEK293T cells (**Fig. 1B**). Although CD43-HEK293T cells were spherical and detached from plates, we found these cells not dead or apoptotic by Trypan-blue staining and by nucleic acid staining (data not shown). No significant accumulation in mitotic phase was observed in CD43-HEK293T cells (**Fig. 1C**), either.

Since CD43 is a well-documented inhibitor for cell adhesion, we presumed these alterations in cell shape were caused by the loss of cell-substrata adhesion. To confirm such effects of CD43 on cell adhesion in HEK293T cells, we developed HEK293T cells stably expressing human α4 integrin (α4-HEK293T) as well as plates coated with GST fusion protein of fibronectin CS1 peptide (GST-CS1), a ligand for α4β1 integrin. α4-HEK293T cells bind and spread on BSA-blocked GST-CS1-coated plates, while HEK293T cells do not (**Sup. Fig. 1A**). Expression of CD43 in α4-HEK293T cells inhibited cell adhesion and spreading on BSA-blocked GST-CS1-coated plates (**Sup. Fig. 1B–D**),

indicating CD43's inhibitory effect on integrin-mediated cell adhesion in HEK293T cells.

Identifiation of microvilli-like protrusions in CD43-HEK293T cells. In addition to cell rounding and inhibition of cell adhesion by CD43, we also noticed cell surface protrusions in CD43-HEK293T cells. Fluorescence of CD43-mCherry fusion protein was observed at the structures protruding from edges of round cell bodies by live cell investigation (**Fig. 2Ab** and arrows). To further study these protrusions, CD43-GFP-HEK293T cells were detached by pipetting, reattached to PLL-coated coverslips, fixed and investigated by fluorescent microscopy. As demonstrated in **Figure 2B**, fine long protrusions were visualized as the fluorescence of CD43-GFP.

For the precise investigation of these protrusions, CD43-HEK293T cells attached to PLL-coated coverslips were analyzed by immunocytochemistry. As demonstrated in **Figure 2Ca**, CD43 (green), visualized by anti-CD43 mAb, was observed in part at cell surface protrusions. Meanwhile, filamentous actin (red), visualized by AF546-labeled Phalloidin, was also identified at protrusions (**Fig. 2Cb**) and co-localized with CD43 (merged image, **Fig. 2Cc**). Ezrin, one of known microvilli-localizing proteins,[34] was also detected at the protrusions in CD43-HEK293T cells (**Fig. 2Cd–f**). These findings indicated that there are microvilli-like protrusions rich in CD43, filamentous actin and Ezrin in CD43-HEK293T cells.

For further analysis of these protrusions, we investigated CD43-HEK293T cells by electron microscopy. Many long protrusions were observed by SEM and by ultrathin-section electron microscopy in CD43-HEK293T cells (**Fig. 2Db and d**, respectively), while a few short protrusions were observed in Vector-HEK293T cells (**Fig. 2Da and c**). Parallel fibers of filamentous actin were observed within such protrusions by ultrathin-section electron microscopy (**Fig. 2De and f**, arrows), confirming these protrusions as microvilli. It was also observed that glycocalyx in the surface of microvilli was thick in CD43-HEK293T cells, whereas thin in Vector-HEK293T cells (**Fig. 2De and f**, arrowheads).

Given the fact that CD43-HEK293T cells were surrounded by microvilli, we wondered subcellular localization of adhesion molecules such as integrin. Immunocytochemical analysis with anti-integrin mAbs demonstrated that both α4 and β1 integrin were localized at the protrusions in CD43-α4-HEK293T cells (**Fig. 2E**). Thus, although integrin-mediated cell adhesion was defective in these cells, integrin was localized on cell surface microvilli.

Augmentation of microvilli-like protrusions by CD43 expression. Although we found long microvilli in CD43-GFP-HEK293T cells, we did not know whether CD43 induced augmentation of such protruding structure, or, was just localized at such structure already existing in HEK293T cells. To determine the effect of CD43 on augmentation of microvilli, we attempted to visualize cell membrane by fluorescent microscopy to investigate cell surface microstructure.

First, we tried to visualize cell membrane by a fluorescent probe for membrane. Cells attached to PLL-coated coverslips were incubated with Cell Mask Orange (CMO) (Invitrogen) for

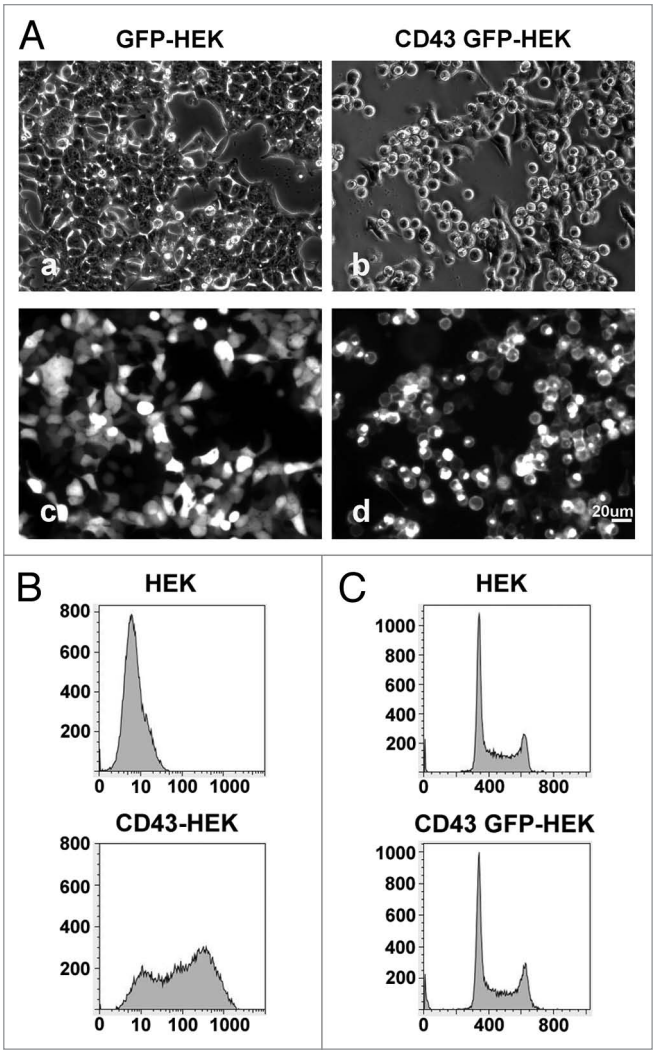

Figure 1. Alterations in cell morphology by the expression of CD43. (A) Phase-contrast (a and b) and fluorescent images (c and d) of HEK293T cells transfected with GFP expression vector (a and c) or CD43-GFP expression vector (b and d). (B) FCM analysis of cell surface CD43 with anti-CD43 mAb. (C) Cell cycle analysis of CD43-HEK293T cells by FCM with Propidium Iodide.

5 min, washed, fixed and analyzed by fluorescence microscopy. In CD43-GFP-HEK293T cells, long protrusions were visualized by the fluorescence of CD43-GFP and by that of CMO (**Fig. 3Ad and b**), indicating that microvilli-like protrusions were visualized by the staining with CMO. In contrast, short cell surface protrusions were identified as the fluorescence of CMO in HEK293T cells (**Fig. 3Aa**). Although this method was easy and no need of transgene, fluorescence of CMO at protrusions was weak. Therefore, we next tested membrane-anchored fluorescent proteins to visualize cell surface microstructure. mCherry fused to the myristoylation site of c-Src (Myr-mCherry) was co-expressed with either GFP or CD43-GFP and localization of fluorescent proteins were investigated. In CD43-GFP-HEK293T cells, long and dense protrusions were identified by Myr-mCherry (**Fig. 3Bb**) at the same sites as CD43-GFP (**Fig. 3Bd**), indicating that microvillous protrusions were

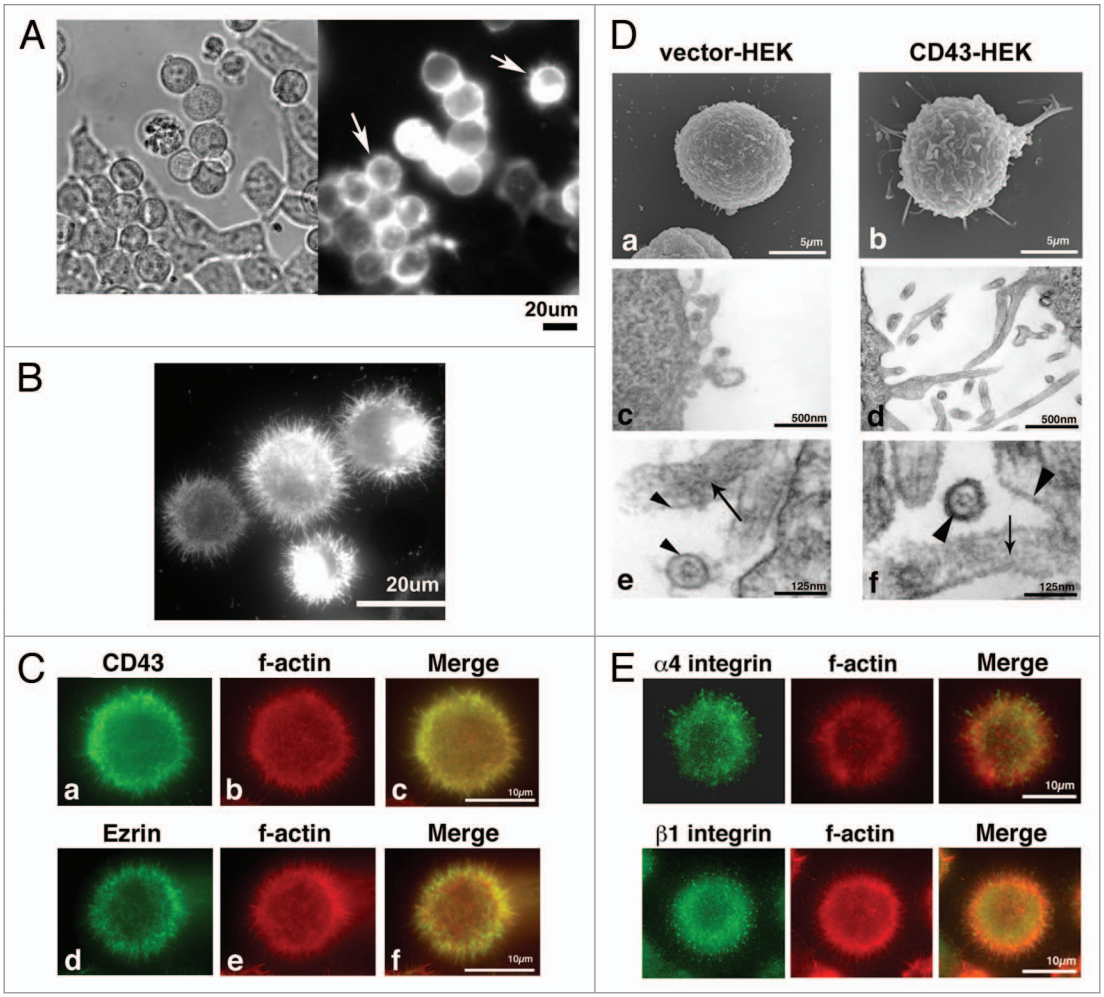

Figure 2. Localization of CD43 at microvillous protrusions. (A) Subcellular localization of CD43-mCherry. A phase contrast and a fluorescent image of CD43-mCherry-HEK293T cells cultured in a plate were presented. Arrows indicate cells with protrusions. (B) Subcellular localization of CD43-GFP in CD43-GFP-HEK293T cells fixed on a PLL-coated coverglass. (C) Subcellular localizations of CD43 and Ezrin in CD43-HEK293T cells. CD43-HEK293T cells fixed on PLL-coated coverglasses were double stained with anti-CD43 mAb (a) or anti-Ezrin mAb (d) and AF546-phalloidin (b and e). Merged images were shown in (c and f). (D) Electron microscopy of HEK293T transfectants. Scanning electron micrographs of Vector-HEK293T (a) and CD43-HEK293T cells (b). Ultrathin-section electron micrographs of Vector-HEK293T (c and e) and CD43-HEK293T cells (d and f). Arrows indicate actin filaments. Arrowheads indicate lipid bilayer membranes. (E) Subcellular localization of integrin in CD43-α4-HEK293T cells. Fluorescent images of immunocytochemistry with anti-α4 integrin mAb (a) or anti-β1 integrin mAb (d) and AF546-phalloidin (b and e) were presented. Merged images were shown in (c and f).

visualized by the fluorescence of Myr-mCherry. In contrast, short and sparse protrusions were identified at the surface of GFP-HEK293T cells by Myr-mCherry (**Fig. 3Ba**).

These analyses revealed augmentation of the number and length of cell surface microvilli-like protrusions by CD43. However, cell surface structure might be changed during detachment, re-attachment, or fixation. Therefore, we next attempted to visualize microstructure of live cell surface. α4-HEK293T cells expressing either Myr-GFP or CD43-GFP were cultured in GST-CS1-coated coverglass chambers, and were scanned by laser confocal microscopy. Fluorescence of either Myr-GFP or CD43-GFP in each Z phase was presented in **Figure 3C**. In Myr-GFP-α4-HEK293T cells, Myr-GFP was detected as hand-like structure with finger-like protrusions at the bottom and attachment phase, while was detected as short protrusions at the top phase. At the middle phase, Myr-GFP was mostly detected as smooth membrane and was hardly detected as protrusions. In contrast, CD43-GFP was observed as long protrusions and surface edge at every phase in CD43-GFP-α4-HEK293T cells. CD43-GFP cells were spherical and taller than Myr-GFP cells, attached to the coverglass with smaller area compared to Myr-GFP cells. These observations further demonstrated augmentation of microvilli around whole cell surface in CD43-HEK293T cells. To digitalize the effect of CD43 on microvilli formation, we took fluorescent images of live Myr-mCherry-HEK293T cells and CD43-mCherry-HEK293T cells at the middle phase, and measured the number and length of microvilli in these images. As the result, the number of microvillous protrusions per cell in each image was 1.99 ± 2.23 (mean value ± standard deviation) for Myr-mCherry-HEK293T, while 32.4 ± 13.7 for

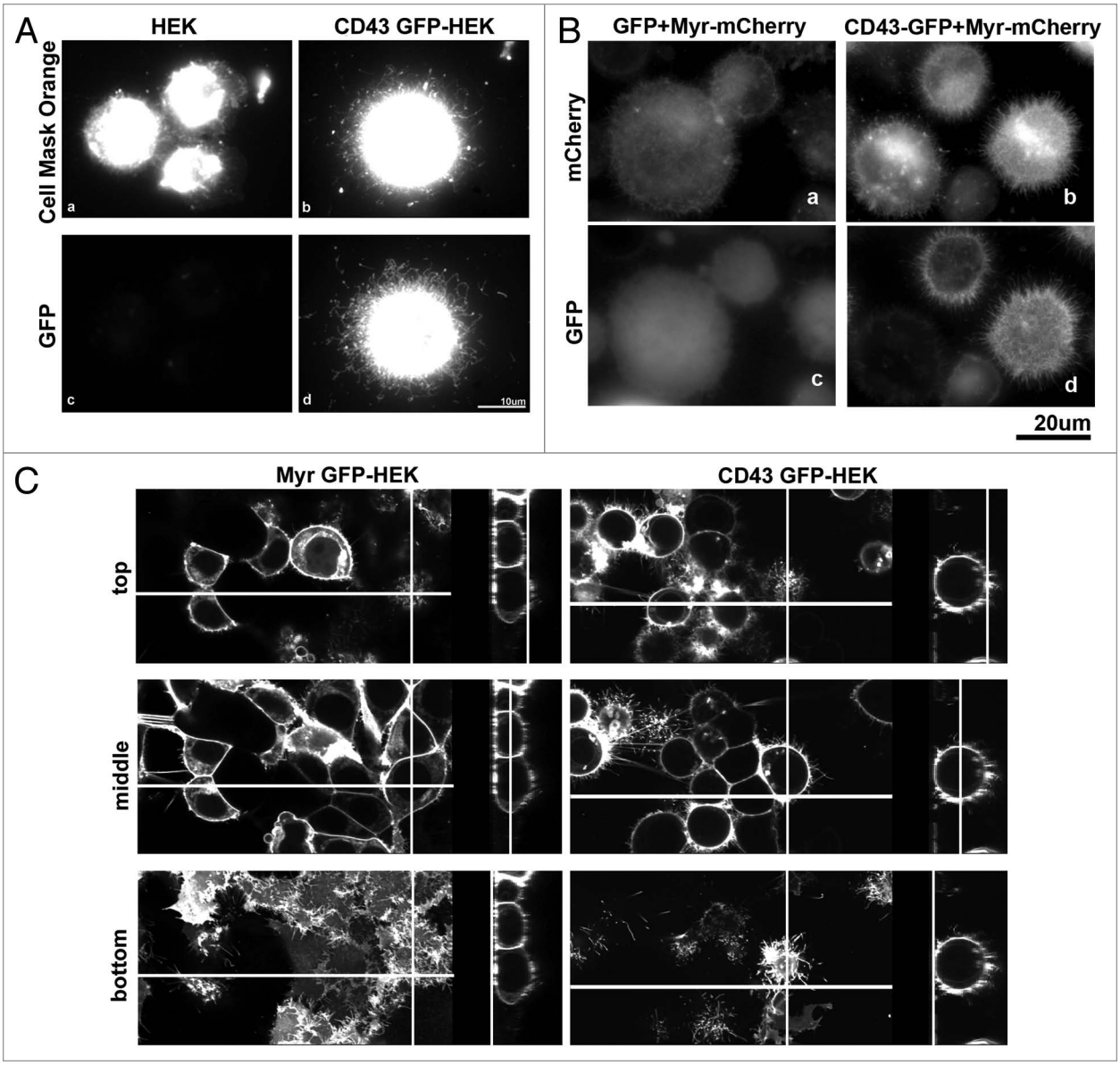

Figure 3. Augmentation of Microvillous protrusions by CD43 expression. (A) Visualization of cell surface protrusions by membrane staining. HEK293T (a and c) and CD43-GFP-HEK293T (b and d) cells re-plated on PLL-coated cover slips were briefly incubated with Cell Mask Orange before fixation and were investigated by fluorescent microscopy. (B) Visualization of cell surface protrusions by myristoylated mCherry (Myr-mCherry). Myr-mCherry was co-expressed with either GFP or CD43-GFP in HEK293T cells. Cells were detached, re-attached to PLL-coated coverslips, fixed and investigated by fluorescent microscopy. (C) Confocal microscopic analysis of CD43-GFP and Myr-GFP. Live cell images of Myr-GFP-HEK293T and CD43-GFP-HEK293T cells in coverglass chambers were captured by confocal laser scanning microscopy. Three scanned images of different phases and Z-stack images for each cell were presented. Lines show the sections where the side images represent.

CD43-mCherry-HEK293T cells. Meanwhile, the length of protrusions is 1.2 ± 0.85 μm for Myr-mCherry-HEK293T, while 3.30 ± 1.83 μm for CD43-mCherry-HEK293T cells. These digitalized results further show augmentation of both quantity and length of microvilli by CD43 expression.

Search for the CD43 domains essential for cell rounding and adhesion. Then, how CD43 induces cell rounding and formation of microvilli? It was proposed that inhibition of cell adhesion is mediated by the ectodomain of CD43.[17] Meanwhile, it is reported that the intracellular domain of CD43 is responsible for its localization and potential formation of microvilli.[31,32] Therefore, we next investigated which domain of CD43 was essential for the alterations of cell morphology.

For this purpose, we first investigated GFP fusion protein of CD44, another ERM-binding protein.[44] If the addition of transmembrane adaptor proteins for ERM is sufficient to induce alterations in cell morphology, forced expression of CD44 should induce such changes. As the result, although CD44-GFP was expressed on cell surface, CD44-GFP expression did not induce cell rounding (**Fig. 4Aa**). Then, to determine CD43 domains essential for morphological alterations, we analyzed chimeric molecules between CD43 and CD44. A chimeric protein composed

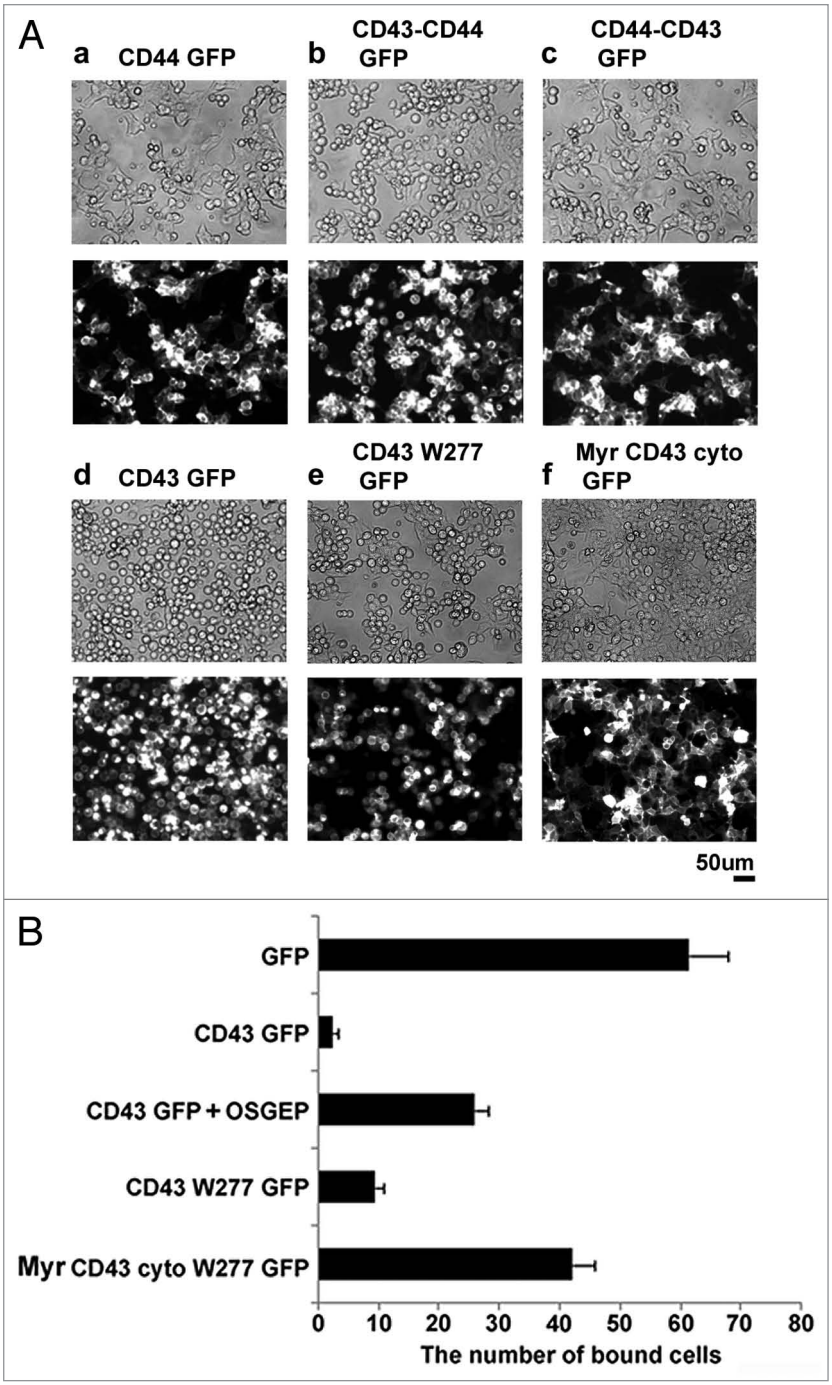

Figure 4. CD43's domain essential for cell rounding and inhibition of cell adhesion. (A) Effects of CD44 and CD43 mutants on cell morphology. GFP fusion protein of CD44 (a), CD43-CD44 chimera (b), CD44-CD43 chimera (c), CD43 (d), CD43 extracellular and transmembrane domains (CD43W277, e), or myristoylated CD43 cytoplasmic domain (Myr-CD43cyto, f) was expressed in HEK293T cells. Cell shape and subcellular localization of GFP fusion protein on the culture plates were visualized by phase contrast (top) and fluorescent (bottom) microscopy. (B) Effect of CD43 mutant on integrin-mediated cell adhesion. Each histogram indicates the number of fluorescent cells adhered to GST-CS1-coated surface from three experiments. For OSGEP treatment, CD43-GFP-α4-HEK293T cells were incubated with OSGEP for 5 h before assay.

of the CD43 ectodomain and the transmembrane and intracellular domains of CD44 induced cell rounding (**Fig. 4Ab**), while a chimeric protein of the CD44 ectodomain and the transmembrane and intracellular domains of CD43 did not (**Fig. 4Ac**). To further define CD43 domains essential for cell rounding, we next analyzed deletion mutants of CD43. CD43W277-GFP, which lacks the entire CD43 cytoplasmic domain, induced cell rounding and detachment (**Fig. 4Ae**), like CD43-GFP (**Fig. 4Ad**). Although CD43W277-GFP appeared to be less effective compared to CD43-GFP, this relative ineffectiveness may be due to the slower localization of CD43W277-GFP to cell surface. Meanwhile, the membrane-anchored CD43 cytoplasmic domain (Myr-CD43cyto-GFP) did not induce such cell shape alterations (**Fig. 4Af**). Thus, the membrane-anchored extracellular domain of CD43 is sufficient for cell rounding, while the CD43 cytoplasmic domain is not essential.

Next, we investigated the effects of CD43 mutants on cell adhesion by the integrin-mediated binding assay described before. α4-HEK293T cells expressing GFP or Myr-CD43 cytoplasm-GFP were bound to the GST-CS1-coated substrata, while cells expressing CD43-GFP or CD43W277-GFP were mostly not bound (**Fig. 4B**). Moreover, treatment of CD43-GFP-α4-HEK293T cells with *O*-Sialoglycoprotein Endopeptidase (OSGEP) (Cedarlane Laboratories, Burlington, NC USA), a bacterial peptidase that cleaves the extracellular peptides of sialomucins, partially augmented attachment of cells to the CS1-coated substrata. These results indicate that the ectodomain is essential and sufficient for the inhibition of integrin-mediated cell adhesion by CD43.

To confirm the effects on integrin-mediated cell adhesion, α4-HEK293T cells and CD43 transfectants were trypsinized and re-attached to GST-CS1-coated plates. Cellular lysates were prepared from these cells after incubation, and were subjected to immunoblotting with anti-phospho-FAK Ab. As demonstrated in **Figure 5**, phosphorylation of FAK-Y397 was augmented by the incubation of α4-HEK293T cells in the CS1-coated substratum. However, augmentation of phosphorylated FAK was largely reduced in CD43-α4-HEK293T and CD43W277-α4-HEK293T cells. Since tyrosine phosphorylation of FAK-Y397 is the major downstream signaling of integrin-mediated cell adhesion, this result further confirm inhibition of integrin-mediated cell adhesion by CD43 or by CD43W277 in HEK293T cells.

Involvement of the CD43 ectodomain in the formation of protrusions. Next, to determine the

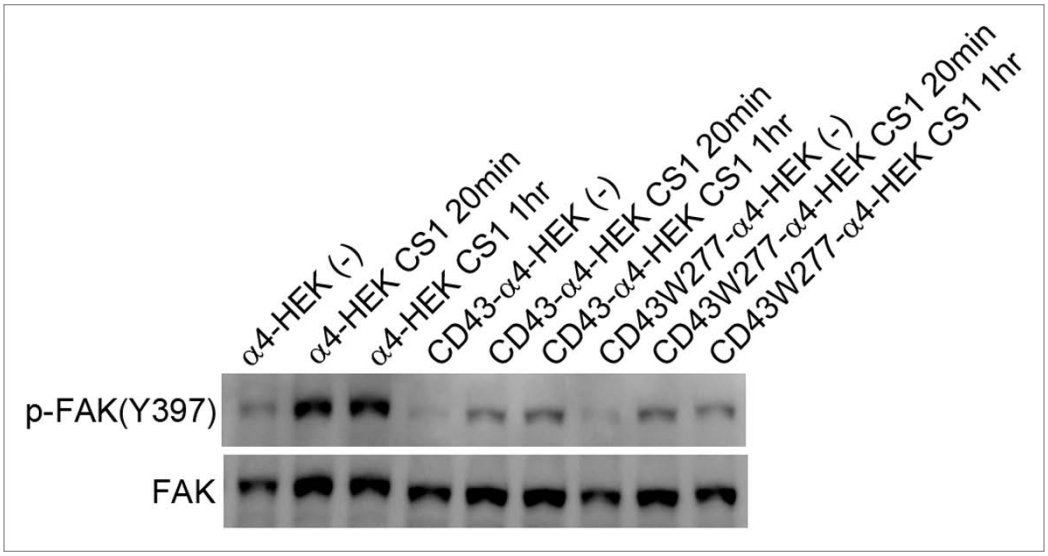

Figure 5. Decreased integrin-mediated phosphorylation of FAK by CD43 expression. CD43-GFP or CD43W277-GFP was expressed in α4-HEK293T cells. These transfectants and α4-HEK293T cells were trypsinized, washed and re-plated onto CS1-coated dishes and incubated for indicated time and then, lyzed. Cellular lysates were subjected to SDS-PAGE and immunoblotting with anti-phospho-FAK [pY397] Ab or anti-FAK mAb.

CD43's domains essential for microvilli formation, we investigated GFP fusion proteins in live cells at the bottom phases in coverglass chambers. As the result, CD43-CD44-GFP, CD43-GFP and CD43W277-GFP were observed as long microvillous protrusions (**Fig. 6Ab, d and e**, respectively). Meanwhile, CD44-GFP, CD44-CD43-GFP, and Myr-CD43cyto-GFP were detected as short protrusions or as a flat membranous pattern (**Fig. 6Aa, c and f**). Myr-CD43cyto-GFP was also detected as hand-like structure with finger-like protrusions at the edge.

To further define microvilli formation by CD43 mutants, we performed live cell investigation by confocal microscopy. As demonstrated in **Figure 6B**, HEK 293T cells expressing Myr-CD43cyto-GFP were flat, while cells expressing CD43W277-GFP were spherical and taller. Myr-CD43cyto-GFP was found as hand-like structure with finger-like protrusions at the bottom, as short sparse protrusions at the top, and as smooth membranous structure in the middle. Thus, while localized close to cell surface, Myr-CD43cyto-GFP, like Myr-GFP, was not identified as long microvillous protrusions. Meanwhile, long protrusions were found at every phase in CD43W277-GFP cells. Thus, expression of CD43W277-GFP, but not Myr-CD43cyto-GFP, induced formation of microvilli-like long protrusions, although microvilli formation in CD43-GFP cells (**Fig. 3C**) was more evident that that in CD43W277-GFP cells. These results indicate that the ectodomain is essential and sufficient for the microvilli formation by CD43. Meanwhile, the cytoplasmic domain is not sufficient or essential for microvilli formation, although might contribute to some extent. In addition, since CD43W277-GFP was detected at microvilli, the cytoplasmic domain is not essential for the localization of CD43 at microvilli. Thus, the direct association of the CD43's cytoplasmic domain with ERM is not the major mechanism for CD43 to induce microvilli formation, cell rounding and inhibition of cell adhesion.

Augmentation of microvilli occured in prior to rounding of CD43 transfectants. Both cell rounding and microvilli formation were induced by the ectodomain of CD43, strongly suggested a relation between these two events. To investigate this relation, live cell imaging of altering cell morphology and microvilli formation was performed in CD43-mCherry-HEK293T cells cultured in a coverglass chamber. **Figure 7A** showed the same cells with an interval of 4 h. CD43-mCherry-HEK293T cells changed their spreading morphology (**Fig. 7A a, c, 1–3**) to more spherical one (**Fig. 7Ab and d**) in 4 h, while a HEK293T cell with little CD43-mCherry expression (**Fig. 7A4**) maintained a similar cell shape. When cells became spherical, cellular structures bridging substrata-attachment sites (**Fig. 7A**, triangles) and cell bodies were either lost (**Fig. 7Ab1**) or diminished (**Fig. 7Ab, 2 and 3**), while cell-cell attachments were also lost (**Fig. 7Ab**, arrows). CD43-mCherry was observed at retracting end (**Fig. 7Ad**, arrowheads) and around the vanishing cell-cell attachment sites (**Fig. 7Ad,** arrows), further suggesting the involvement of CD43 in the inhibition of cell adhesion. Interestingly, CD43-mCherry had been already observed as microvilli-like protrusions at the attachment phase before cell rounding (**Fig. 7Ac, 1–3**).

Since CD43-rich protrusions were observed in prior to cell rounding, we intended to investigate localization of CD43 in earlier phases. At an earlier time point, when cells were still spread, CD43-mCherry was localized diffusely at cell membrane (**Fig. 7Ba**, arrows) and at long or short protrusions (**Fig. 7Bb and c**, arrowheads) at the bottom phase.

Next, we performed a time-lapse experiment to further investigate the transition of CD43 localization. As demonstrated in **Figure 8**, a CD43-mCherry-HEK293T cell (left, upper) was transformed from square to spindle-like shape in 3 h. During this period, CD43-mCherry diffusely localized at cell membrane (arrows) disappeared, while short protrusions (arrowheads) appeared. Long protrusions had been also observed at the sites

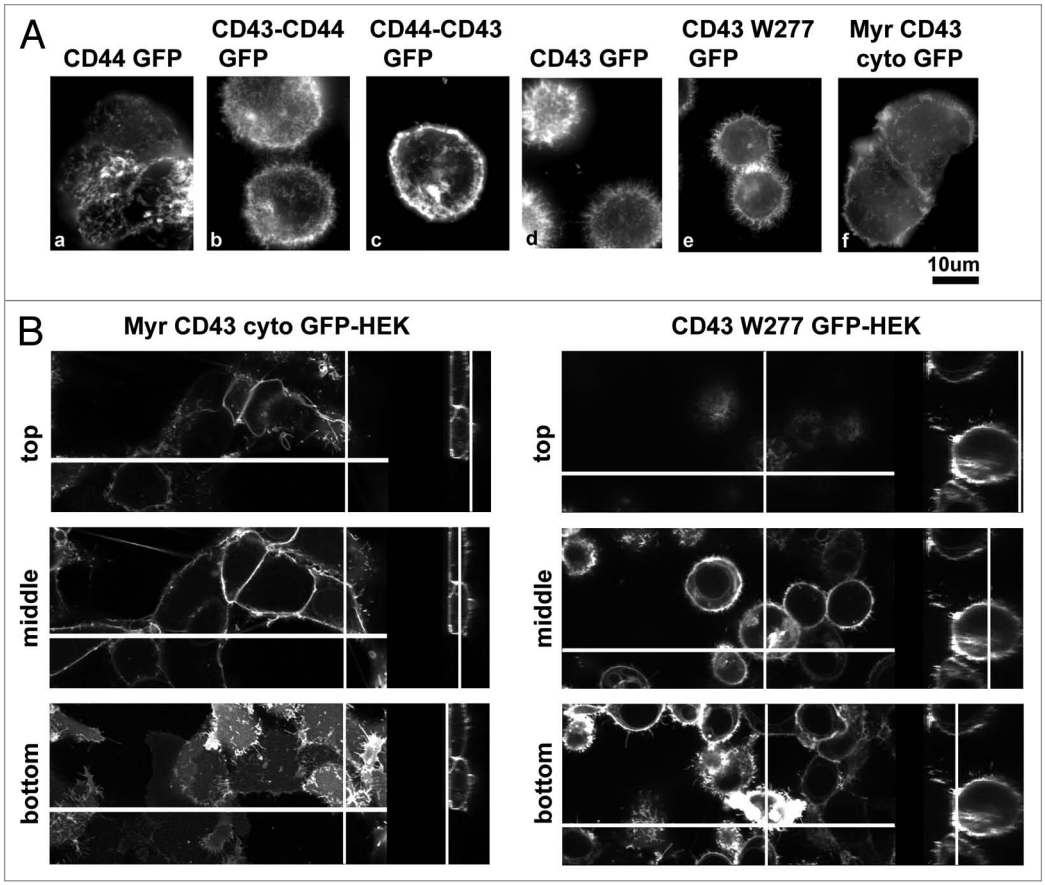

Figure 6. CD43's domain essential for microvilli formation. (A) Effect of CD44 and CD43 mutants on microvilli formation. HEK293T transfectants cultured in coverglass chambers were investigated by fluorescent microscopy. Expressed proteins were same as Figure 4A. (B) Confocal microscopic analysis of CD43 mutants. Live cell images of Myr-CD43cyto-GFP-HEK293T and CD43W277-GFP-HEK293T cells in coverglass chambers were captured by confocal microscopy. The method to present images was identical as Figure 4C.

where cell body was later retracted. These findings strongly suggested that cell rounding was accompanied with formation of microvilli-like protrusions.

Augmented phosphorylation of ERM by CD43. Then, what's the mechanism that induces microvilli formation and cell rounding? Because ERM, especially phosphorylated ones, are localized at microvilli, Uropods and cortex of rounded cells,[12,31,34-36,41,42] we were interested in ERM and their regulation and studied phosphorylation of ERM by CD43 expression.

First, HEK293T transfectants were investigated by immunocytochemistry with anti-phospho-ERM Ab. As demonstrated in **Figure 9A**, immunostaining with anti-phospho-ERM Ab at microvillous protrusions was largely augmented in the cells expressing CD43GFP or CD43W277GFP compared to that in Myr-GFP cels. Phosphorylated ERM were also detected at the cortex of cells, especially at the roots of protrusions, in CD43-GFP and CD43W277-GFP cells. To confirm augmenteation of phosphorylated ERM, we analyzed lysates of transfectants by immunoblotting. Phosphorylated ERM were clearly augmented in CD43-GFP and CD43W277-GFP cells, while marginally augmented in Myr-CD43cyto-GFP cells, compared to those in HEK293T cells (**Fig. 9B**). Thus, ectodomain of CD43 was again essential and sufficient for the phosphorylation of ERM by CD43.

Next, to further define the relation between CD43 and ERM phosphorylation, we investigated phosphorylated ERM in the early stages of CD43 expression. As demonstrated in **Figure 9C**, phosphorylated ERM were detected co-localized with CD43-GFP at protrusions (arrowheads). In contrast to the sites of protrusions, phospho-ERM were not detected at the sites where CD43-GFP was observed as a diffuse membranous pattern (arrows). These results further suggested that phosphorylation of ERM was accompanied with the formation of protrusions by CD43 even in the early stages.

Cell detachment induces phosphorylation of ERM. Then, how did CD43's ectodomain induce phosphorylation of ERM? Since CD43 is an inhibitor for cell adhesion, we presumed that inhibition of cell adhesion induces phosphorylation of ERM. To define this possibility, HEK293T cells were detached from substrata by trypsinization and incubated in BSA-coated plates with gentle swirling to inhibit re-attachment. Then, the lysates of such cells were analyzed by immunoblotting with anti-phospho-ERM Ab. As demonstrated in **Figure 10A**, phosphorylated ERM were augmented in the lysates of detached cells, suggesting induction of ERM phosphorylation by keeping adherent cells detached from substrata. To further define this possibility, a similar analysis was performed using α4-HEK293T cells with or without

re-attachment to GST-CS1-coated substrata. Cell detachment by trypsin and following washing procedure induced ERM phosphorylation (**Fig. 10B**, pellet). Keeping cells detached from substrata further augmented phosphorylated ERM (**Fig. 10B, BSA**), while re-attachment to the CS1-coated plates significantly decreased phoshorylated ERM (**Fig. 10B, CS1**). Thus, detachment of cells from substrata and inhibition of re-attachment induce phosphorylation of ERM in HEK293T cells. Taken together, our findings indicate the possibility that inhibition of cell adhesion by CD43 induces ERM phosphorylation, which is accompanied with microvilli formation and eventual cell rounding.

Discussion

In this article, we have demonstrated CD43 expression induces cell shape alterations, both augmentation of microvilli and a switch from a polarized to spherical shape, inhibits integrin-mediated and cell-cell re-attachments and augments phosphorylated ERM in HEK293T cells. Mutant studies showed the ectodomain of CD43 was essential and sufficient for all these phenomena, strongly suggesting relations between these events. We would like to argue such relations and potential mechanisms how CD43 induces these phenomena.

CD43 and microvillous protrusions. Previously, CD43 was linked to microvilli by two subjects, localization of CD43 in microvilli-like protrusions,[31] and augmentation of microvilli by the expression of E-cadherin-CD43 chimera.[32] In the latter case, CD43 was considered as an adaptor protein that recruits ERM and links membrane and actin cytoskeleton, but was not considered as an activator for ERM. However, our results using CD43 mutants indicated that the intracellular domain is not essential or sufficient for the induction of microvillous protrusions by CD43. Therefore, adaptor function for the recruitment of ERM is not the major mechanism by which CD43 augments microvilli. Indeed, there should be sufficient amounts of endogenous adaptor molecules for activated ERM in HEK293T cells, since phosphorylated ERM were localized at microvilli in cells expressing CD43W277-GFP, a CD43 mutant lacking the cytoplasmic domain. Meanwhile, CD43W277-GFP was localized at microvilli, indicating that the cytoplasmic domain, and therefore, interaction with ERM, is not essential for the localization of CD43 to microvilli, either. A previous publication about podocalyxin also supported the insignificance of the intracellular domain in microvillous formation.[30]

ERM phosphorylation and CD43-induced alterations in cell morphology. Then, how does CD43 induce augmentation of microvilli by its ectodomain? We found increase in phosphorylated ERM as the result of CD43 expression. Knocking down *ERM* transcripts abrogated microvilli in mouse thymoma cells,[37] indicating ERM as an essential component of microvilli. A phosphorylated form-mimicked mutant of Moesin augmented microvilli in peripheral blood T cells and delayed chemokine-induced loss of microvilli.[26] Taken together, it is highly likely that activated ERM is involved in the formation and maintenance of microvilli. It is better noted that phosphorylation of the C-terminal threonine residue may not be necessary for the activation of ERM as well as microvilli formation in all cell types.[45] However, phosphorylated ERM are specifically observed at microvilli and at the cortex of spherical cells, indicating phosphorylation of this specific site can be considered as a marker for activated ERM.

Meanwhile, phosphorylated ERM were also accompanied with cell rounding. Moesin was phosphorylated at the onset of mitosis in Drosophila cells and knocking down *Moesin* or its kinase, *Slik*, resulted in the inhibition of mitotic cell rounding and reduced cortical rigidity.[42] Phosphorylated ERM were detected at the cortex of spherical circulating leukocytes,[26,41] and dephosphorylation of such ERM was accompanied with a switch from a spherical to a polarized shape upon stimulation of chemoattractants.[12,26,43] Taken together, it is likely that localization of activated ERM at the cortex is essential for the formation and maintenance of a spherical shape and cortical rigidity.

In CD43-GFP-HEK293T cells, phosphorylated ERM were spacially and temporally co-localized with CD43-GFP at

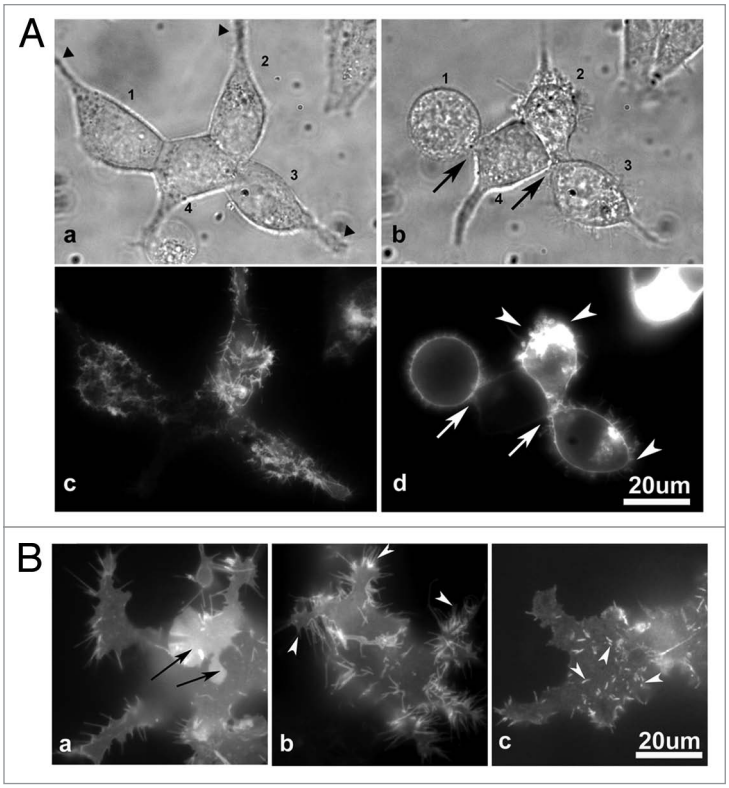

Figure 7. CD43 localization at protrusions in prior to cell rounding. (A) Images of CD43-mCherry-HEK293T cells at two time points. HEK293T cells in a coverglass chamber were transfected with pCpuroCD43-mCherry. Phase contrast cell images (a and b) and fluorescent images of CD43-mCherry (c and d) were captured at 14 and 18 h after transfection. Cells were numbered 1–4. Triangles represented cell-substrata attachment sites. Arrows and arrowheads represented the sites of lost cell-cell and cell-substrata connections, respectively. (B) Fluorescent images of CD43-mCherry at the bottom of spread cells. In an early stage of CD43 expression, CD43-mCherry was detected as diffusely membranous (a, arrows) or as long and short protrusions (arrowheads).

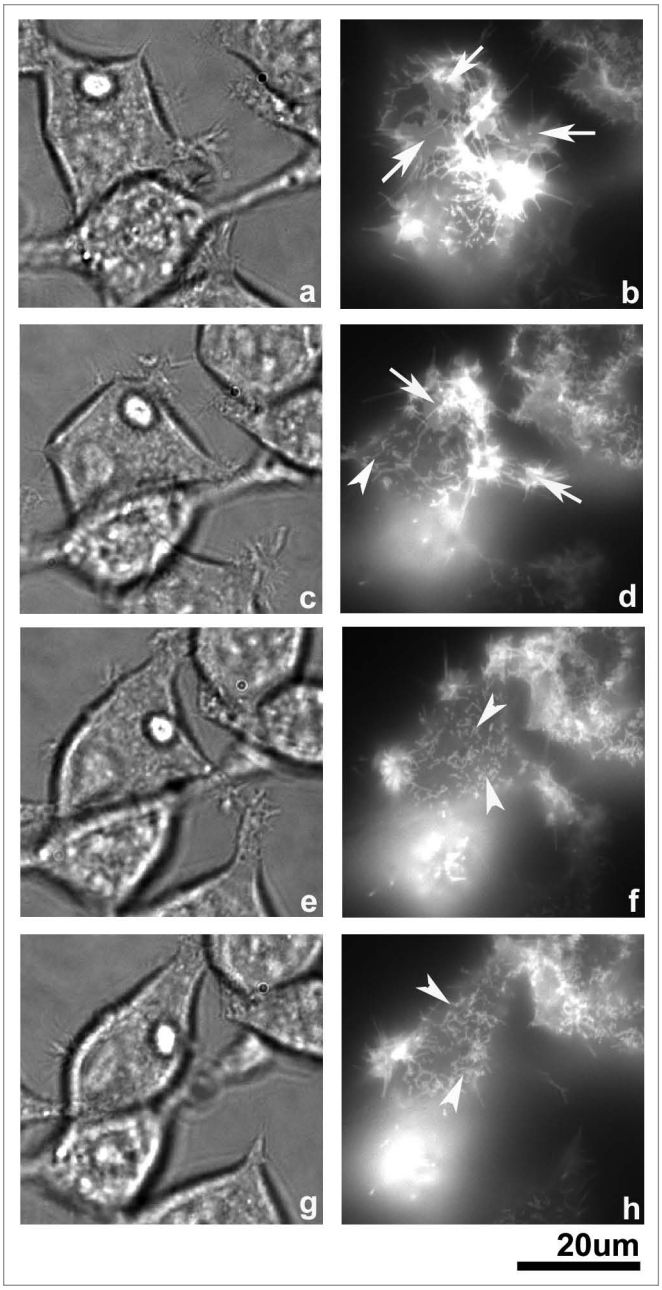

Figure 8. Time-lapse images of CD43-mChery-HEK293T cells in early phases. From top (a and b) to bottom (g and h), images of the same cells were captured started at 16 h after transfection of pCpuroCD43-mCherry with an interval of 1 h each. Diffuse membranous pattern was shown by arrows, while short protrusions were shown by arrowheads.

microvillous protrusions, however, were not identified at the sites where CD43-GFP showed diffusely membranous localization. Phosphorylated ERM were also observed at the cortex of spherical CD43-GFP cells (**Fig. 9A**), but not at the surface of cells still spread (**Fig. 9C** and arrows). Thus, activation and phosphorylation of ERM are accompanied with microvilli formation and cell rounding by CD43, and may be the mechanism of these phenomena.

Cell detachment and ERM phosphorylation. Then, how phosphorylation of ERM is induced by CD43? Mutant assay showed the ectodomain is responsible for this ERM phosphorylation. Possible functions of CD43's ectodomain include (i) the inhibition of cell adhesion, (ii) interaction with other cell surface molecules. To distinguish these CD43's functions, we simply detached parental HEK293T cells by trypsin-EDTA to mimic inhibition of cell adhesion by CD43, and investigated phosphorylation of ERM. As the result, phosphorylated ERM were largely augmented by trypsin-induced cell detachment and by the inhibition of re-attachment, while were reduced by integrin-mediated re-attachment. It is worth noted that this phosphorylation of ERM was not caused by microvilli formation, since detachment of HEK293T cells by trypsin-EDTA does not induce long microvilli observed in CD43 transfectants.

Based on these findings, we propose that inhibition of cell adhesion by the expression of CD43's ectodomain induces phosphorylation of ERM. Given ERM phosphorylation by trypsinization of cells, we believe it more likely than the other mechanism at this moment. Furthermore, if CD43 augments phosphorylated ERM by inducing cell detachment, phosphorylated ERM is likely the cause, not the result, of microvilli formation. Besides CD43, ERM phosphorylation by cell detachment, and/or, ERM dephosphorylation by integrin-mediated cell adhesion, could be a novel mechanism for the organization of actin cytoskeleton and cellular structure in a large variety of cells.

Inhibition of cell adhesion, microvilli formation and cell rounding. As the other relation between CD43-induced events, formation of microvilli was observed in prior to cell rounding. Moreover, these microvilli were observed at the attachment sites that lost attachments later during rounding of CD43-HEK293T cells. The drastic alterations from a spread to a spherical shape within a short period of time (**Figs. 7 and 8**) suggest loss of attachment sites largely contributed to cell rounding. Question is whether such microvilli are involved in the detachments of these cells? Unlike protrusions in Myr-GFP-HEK293T cells, microvilli in CD43-GFP-HEK293T cells appear to be not adhesive to substrata (**Fig. 3C**). CD43-rich microvilli in CD43-HEK293T cells are about 3 μm in average length and about 0.1–0.2 μm in width, considerably larger than the ectodomain of CD43, 0.045 μm in average length.[17] Therefore, if CD43-rich microvilli are generated at or around the sites of attachment, such microvilli will likely induce further detachment of cell body from substrata and from other cells. Such detachment may also activate ERM and activated ERM possibly stabilize spherical shapes of cells.

Taken together, we presume the mechanism of CD43-induced alterations in cell morphology as follows. First, CD43 expressed on cell surface inhibits cell adhesion and induces local detachment. Second, this local detachment induces activation of ERM. Third, activated, i.e., phosphorylated, ERM promote formation of microvilli-like protrusions. Then, such protrusions that are formed at the attachment sites induce further detachment of cells. This detachment induce cell rounding by the loss of cell attachment sites and by further activation of ERM.

Potential functions of CD43 in leukocytes. Then, how these findings are translated in primary cells? CD43 is abundantly expressed in many leukocytes, and is accumulated at the Uropods in migrating leukocytes. Most circulating leukocytes

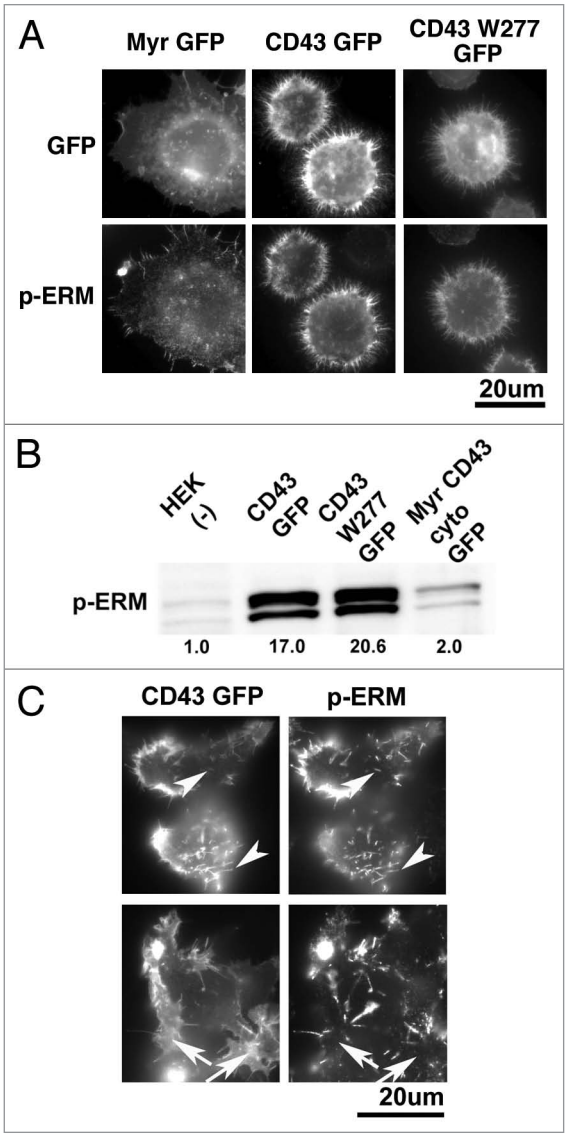

Figure 9. Identification of phosphorylated ERM in CD43-HEK293T cells. (A) Immunocytochemical analysis of phosphorylated ERM. HEK293T transfectants were attached on PLL-coated coverslips, fixed, permeabilized and subjected to immunocytochemical analysis with anti-phospho-ERM Ab. Fluorescent images of GFP fusion proteins and those of phosphorylated ERM were presented. (B) Immunoblot analysis of phosphorylated ERM. Cellular lysates from HEK293T and transfectants were subjected to SDS-PAGE and immunoblotting with anti-phospho-ERM Ab. Relative intensity of phospho-ERM on each lane, modified by that of ERM, was demonstrated as a digital number. (C) Co-localization of phosphorylated ERM with CD43 at microvillous protrusions. HEK293T cells in a coverglass chamber at 14 h after transfection of pCpuroCD43-GFP were fixed, permeabilized and subjected to immunocytochemical analysis with anti-phospho-ERM Ab. Phosphorylated ERM were co-localized with CD43-GFP at protrusions (arrowheads). Meanwhile, phosphorylated ERM were not detected at the sites where CD43-GFP was diffusely localized (arrows).

are spherical and relatively rigid and phosphorylated ERM at the cortex are important for cells to keep their spherical shape and rigidity.[12,41-43] Given inhibition of cell adhesion and following phosphorylation of ERM, we propose CD43 is involved in the formation and maintenance of a spherical shape and rigidity for spherical leukocytes and their Uropods. On the other hand, dephosphorylation of ERM and redistribution of filamentous actin were accompanied with polarization of leukocytes by chemoattractants and other stimuli.[12,41,43] Exclusions of CD43 from the leading edge of polarized cells and from attachment sites further suggest possible function of CD43 in cell rounding.[11-14]

Meanwhile, several adhesion molecules are localized, if not enriched, in leukocyte microvilli.[22,24,25,29] We also observed localization of α4β1 integrin in microvilli in CD43-HEK293T cells. However, those CD43 transfectants were defective in α4β1 integrin-mediated cell adhesion despite localization of integrin in cell surface microvilli. It is conceivable that CD43, rich in microvilli in CD43-HEK293T cells, may inhibit cell adhesion mediated by the molecules located on microvilli. Otherwise, α4β1 integrin in microvilli may be inactive. In either case, it needs further study, because publications suggested augmentation of cell adhesion by the molecules located on leukocyte microvilli.[22] Meanwhile, dephosphorylation of ERM and redistribution of filamentous actin upon chemokine stimulation suggest remodeling of microvilli, as well as that of cortical rigidity, is essential for leukocyte migration and extravasation.[12,26,43] Therefore, it is possible that leukocyte microvilli are a structure that stocks adhesion molecules in inactive forms. These stocked adhesion molecules become active for cell adhesion when microvilli are remodeled by stimulations.

Besides CD43, there are other sialomucins expressed in leukocytes. We have similar results with a few of these sialomucins as those with CD43 (publication in preparation). Therefore, the functions of CD43 demonstrated in this article could be shared in a few other sialomucins and such sialomucins may also play significant roles in the regulation of leukocyte's circulation and migration.

In summary, the ectodomain of CD43 induces phosphorylation of ERM and alterations in cell morphology. Formation of microvilli and rounding of cells are accompanied with ERM phosphorylation, and ERM phosphorylation appears to be induced by the inhibition of cell attachment by CD43. Further studies are necessary for the functions of CD43 in leukocytes and for the mechanism of ERM phosphorylation by cell detachment.

Materials and Methods

Reagents and antibodies. Poly-L-lysin (PLL), puromycin, paraformaldehyde (PFA) and bovine serum albumin (BSA) were obtained from Sigma (St. Louis, MO USA). Monoclonal antibodies, anti-β1 integrin (MAR4), anti-α4 integrin (9F10), anti-Ezrin and anti-FAK mAbs were obtained from BD Biosciences (San Jose, CA USA) and anti-CD43 (L10) mAb was from eBioscience (San Diego, CA USA). Rabbit antibodies, anti-phospho-ERM (#3149) and anti-ERM (#3142) were obtained from Cell Signaling Technologies Inc., (Danvers, MA USA), while rabbit anti-phospho-FAK [pY397] Ab, AF488-labeled goat anti-mouse IgG Ab, AF546-labeled goat anti-rabbit IgG Ab and AF546-labeled Phalloidin were from Invitrogen (Carlsbad, CA USA).

DNAs, cell culture and transfection. cDNAs of human CD43, CD44 transcript variant 4 and α4 integrin were cloned

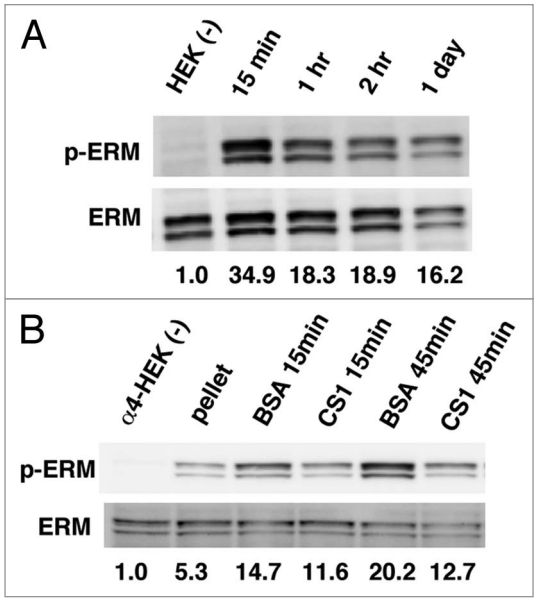

Figure 10. Phosphorylation of ERM by cell detachment. (A) Augmentation of phosphorylated ERM by cell detachment. HEK293T cells were trypsinized, washed and incubated in BSA-coated plates with gentle swirling. Lysates from such cells were subjected to immunoblot analysis with anti-phospho-ERM and anti-ERM Abs. Relative intensity of phospho-ERM on each lane, modified by that of ERM, was demonstrated as a digital number. (B) Decrease of phosphorylated ERM by cell adhesion. α4-HEK293T cells were detached by trypsinization, washed and incubated either in BSA-coated plates with swirling or in GST-CS1-coated plates for indicated time. Lysates from such cells were subjected to the immunoblot analysis described above.

by RT-PCR. Truncated or chimeric DNA fragments were generated from these cDNAs by PCR, fused to the DNA fragment of EGFP or mCherry (Clontech, Mountain View, CA USA) and subcloned into pCpuroCMVS, a retrovirus expression vector generated from pCLNCMV (Imgenex, San Diego, CA USA), or pJ3SrcMS, an expression vector with the myristoylation site of c-Src. HEK293T cells were cultured in Dulbecco's modified Eagle's medium (DMEM) supplemented with 10% fetal calf serum. If not specifically described, cells at 40–44 h after transfection with LipofectAmine 2000 (Invitrogen) were used for analysis. α4 integrin-HEK293T cells were developed by the transfection of pCpuroCMVS-α4 integrin followed by puromycin selection. A bacterial expression vector, pGEX-CS1, which encodes a glutathione S-transferase (GST)-fusion protein of fibronectin CS1 peptide, was a kind gift of Dr. Kenjiro Kamiguchi.[46]

Fluorescence microscopy. For the images of fluorescent proteins in low magnification, transfectants cultured in plastic plates were analyzed by fluorescent microscopy (IX70, OLYMPUS, Tokyo, Japan). For images in high magnification, transfectants were detached, reattached to PLL-coated cover slips, fixed with 4% PFA in phosphate buffered saline (PBS), mounted with Mowiol 4-88 (CALBIOCHEM, Darmstadt, Germany) and analyzed. Otherwise, transfectants cultured in coverglass chambers (Asahi Glass Co., Ltd., Tokyo, Japan) were directly analyzed by fluorescent microscopy. During time-lapse analysis, cells were incubated in Stage Top Incubator (Tokai Hit Co., Ltd., Shizuoka, Japan). Photo images of microscopy were arranged with Adobe Photoshop. Confocal laser scanning microscopy was performed by FV1000 (OLYMPUS) and analyzed by FLUOVIEW (OLYMPUS).

For immunofluorescence microscopy, cells attached to PLL-coated cover slips or cultured in coverglass chambers were fixed with 4% PFA in PBS, permeabilized with 0.2% Triton X-100 in PBS and blocked with 1% BSA in PBS. Then, samples were incubated with primary and secondary antibodies in 1% BSA-PBS, washing with PBS between and after, mounted in Mowiol 4-88 and investigated with fluorescent microscopy (IX70 or BX51, OLYMPUS). For digitalization of microvilli, live fluorescent images at the middle phase were taken from 50 each transfectants. Measurement and calculation of the number and length of fluorescent protrusions was performed by Adobe Photoshop and Microsoft Office.

Scanning electron microscopy. Cells were fixed with 1.2% glutaraldehyde (GA) in 0.1 M phosphate buffer (pH 7.2) (PB) overnight, washed with 5% sucrose in PB and attached to PLL-coated coverslips. Then, cells were fixed with 1% OsO_4 in PB for 20 min, dehydrated, critical-point dried, sputter coated with Au-Pd and observed with JSM-5800LV scanning electron microscope (JEOL, Tokyo, Japan).

Ultrathin-section electron microscopy. Cells were fixed with 1.2% GA in PB overnight, washed with 5% sucrose in 0.1 M PB, fixed with 2% GA in PB overnight. After washed with 0.06 M cacodylate buffer (CB), cells were prefixed with 0.5 mg/ml ruthenium red and 1.2% GA in 0.06 M CB overnight, washed with 0.15 M CB and postfixed with a buffer containing 0.5 mg/ml ruthenium red and 1% OsO_4 in 0.06 M CB for 3 h followed by washing with 0.15 M CB. Then, cells were dehydrated through a graded series of ethanol and propylene oxide and embedded in epoxy resin. Ultrathin sections were cut from these samples, stained with uranyl acetate and lead citrate and then observed with Hitachi H7500 transmission electron microscope (Hitachi High-Technologies Corp., Tokyo, Japan).

Binding assays. For integrin-mediated adhesion assay, plates coated with specific ligands for α4β1 integrin were prepared as follows. Tissue culture plates were incubated with PBS containing either 1 μg/ml GST or GST-CS1 for 3 h and blocked with 1% BSA-PBS for 1 h and washed with PBS. Then, α4-HEK293T transfectants were harvested by trypsinization, washed, resuspended in DMEM and plated onto the coated plates. After incubation in CO_2 incubator for 1 h, images of cell spreading were captured by microscopy. Then, plates were washed four times with DMEM and subjected to capturing images and counting numbers of bound cells.

Flowcytometry (FCM). For cell surface expression, HEK293T and transfectants were incubated with antibodies in ice cold 1% BSA-PBS, washed with PBS and fixed with PBS containing 0.5% PFA. For cell cycle analysis, cells were permeabilized with 0.3% Saponin (Sigma) and incubated with 0.05 mg/ml propidium iodide (Sigma) and 0.25 mg/ml RNaseA (Wako, Osaka, Japan). Then, cells were analyzed by FCM with FACS Calibur (BD Biosciences). Visual images were generated with FlowJo (Tree Star, Inc., Ashland, OR).

Immunoblotting. Cells attached to substrata were washed with ice-cold PBS and lysed in 1% Nonidet-P40 lysis buffer,[46] while non-attached cells were collected by centrifugation, washed and lysed with same buffers. After sonication, cellular lysates were centrifuged at 15,000 rpm for 10 min and the supernatants were boiled with lameli buffer. These samples were separated by 9% acrylamide SDS-PAGE, transferred onto nitrocellulose membranes (PROTRAN, Whatman, Dassel, Germany), blocked with 5% Skim Milk in Tris buffered saline (TBS), incubated with first Ab in TBS containing 5% BSA and analyzed by LAS-4000 mini (FUJIFILM Inc., Tokyo, Japan) with Horseradish Peroxidase-conjugated second Ab (GE Healthcare, Buckinghamshire, UK) and chemiluminescence reagent (Western Lightning Plus-ECL, PerkinElmer, Shelton, CT).

Acknowledgements

We thank Dr. Kenjiro Kamiguchi for pGST-CS-1. We also thank Hideki Saito, Youichi Kato, Hiroko Machida and Yoshihiro Katsube for technical help.

This work was in part supported by a grant for New Energy and Industrial Technology Development Organization (NEDO) and by Grants-in-Aid for Scientific Research (KAKENHI 10011601).

Note

Supplementary materials can be found at:
www.landesbioscience.com/journals/celladhesion/article/13908

References

1. Tadokoro S, Shattil SJ, Eto K, Tai V, Liddington RC, de Pereda JM, et al. Talin binding to integrin β tails: a final common step in integrin activation. Science 2003; 302:103-6.
2. Moser M, Legate KR, Zent R, Fässler R. The tail of integrins, talin and kindlins. Science 2009; 324:895-9.
3. Askari JA, Buckley PA, Mould AP, Humphries MJ. Linking integrin conformation to function. J Cell Sci 2009; 122:165-70.
4. Carlsson SR, Fukuda M. Isolation and characterization of Leukosialin, a major sialoglycoprotein on human leukocytes. J Biol Chem 1986; 261:12779-86.
5. Rosenstein Y, Santana A, Pedraza-Alva G. CD43, a molecule with multiple functions. Immunol Res 1999; 20:89-99.
6. Manjunath N, Johnson RS, Staunton DE, Pasqualini R, Ardman B. Targeted disruption of CD43 gene enhances T lymphocyte adhesion. J Immunol 1993; 151:1528-34.
7. Manjunath N, Correa M, Ardman M, Ardman B. Negative regulation of T-cell adhesion and activation by CD43. Nature 1995; 377:535-8.
8. Ardman B, Sikorski MA, Staunton DE. CD43 interferes with T-lymphocyte adhesion. Proc Natl Acad Sci USA 1992; 89:5001-5.
9. Stockton BM, Cheng G, Manjunath N, Ardman B, von Andrian UH. Negative regulation of T cell homing by CD43. Immunity 1998; 8:373-81.
10. Drew E, Merzaban JS, Seo W, Ziltener HJ, McNagny KM. CD34 and CD43 inhibit mast cell adhesion and are required for optimal mast cell reconstitution. Immunity 2005; 22:43-57.
11. del Pozo MA, Sánchez-Mateos P, Nieto M, Sánchez-Madrid F. Chemokines regulate cellular polarization and adhesion receptor redistribution during lymphocyte interaction with endothelium and extracellular matrix. Involvement of cAMP signaling pathway. J Cell Biol 1995; 131:495-508.
12. Sánchez-Madrid F, del Pozo MA. Leukocyte polarization in cell migration and immune interaction. EMBO J 1999; 18:501-11.
13. Soler M, Merant C, Servant C, Fraterno M, Allasia C, Lissitzky JC, et al. Leukosialin (CD43) behavior during adhesion of human monocytic THP-1 cells to red blood cells. J Leukoc Biol 1997; 61:609-18.
14. Shaw AS. Ferming up the synapse. Immunity 2001; 15:683-6.
15. Pallant A, Eskenazi A, Mattei MG, Fournier RE, Carlsson SR, Fukuda M, et al. Characterization of cDNAs encoding human leukosialin and localization of the leukosialin gene to chromosome 16. Proc Natl Acad Sci USA 1989; 86:1328-32.
16. Fukuda M, Tsuboi S. Mucin-type O-glycans and leukosialin. Biochem Biophys Acta 1999; 1455:205-17.
17. Cyster JG, Shotton DM, Williams AF. The dimensions of the T lymphocyte glycoprotein leukosialin and identification of linear protein epitopes that can be modified by glycosylation. EMBO J 1991; 10:893-902.
18. Mooseker MS, Tilney LG. Organization of an actin filament-membrane complex: Filament polarity and membrane attachment in the microvilli of intestinal epithelial cells. J Cell Biol 1975; 67:725-43.
19. Chhabra ES, Higgs HN. The many faces of actin: matching assembly factors with cellular structures. Nat Cell Biol 2007; 9:1110-21.
20. van Ewijk W, Brons NH, Rozing J. Scanning Electron Microscopy of Homing and Recirculating Lymphocyte Populations. Cell Immunol 1975; 19:245-61.
21. Anderson AO, Anderson ND. Lymphocyte emigration from high endothelial venules in rat lymph nodes. Immunology 1976; 31:731-48.
22. von Andrian UH, Hasslen SR, Nelson RD, Erlandsen SL, Butcher EC. A central role for microvillous receptor presentation in leukocyte adhesion under flow. Cell 1995; 82:989-99.
23. Majstoravich S, Zhang J, Nicholson-Dykstra S, Linder S, Friedrich W, Siminovitch KA, et al. Lymphocyte microvilli are dynamic, actin-dependent structures that do not require Wiskott-Aldrich syndrome protein (WASp) for their morphology. Blood 2004; 104:1396-403.
24. Berlin C, Bargatze RF, Campbell JJ, von Andrian UH, Szabo MC, Hasslen SR, et al. α4 integrins mediate lymphocyte attachment and rolling under physiologic flow. Cell 1995; 80:413-22.
25. Singer II, Scott S, Kawka DW, Chin J, Daugherty BL, DeMartino JA, et al. CCR5, CXCR4 and CD4 are clustered and closely apposed on microvilli of human macrophages and T cells. J Virol 2001; 75:3779-90.
26. Brown MJ, Nijhara R, Hallam JA, Gignac M, Yamada KM, Erlandsen SL, et al. Chemokine stimulation of human peripheral blood T lymphocytes induces rapid dephosphorylation of ERM proteins, which facilitates loss of microvilli and polarization. Blood 2003; 102:3890-9.
27. Ager A, Mistry S. Interaction between lymphocytes and cultured high endothelial cells: an in vitro model of lymphocyte migration across high endothelial venule endothelium. Eur J Immunol 1988; 18:1265-74.
28. Okumura S, Muraoka O, Tsukamoto Y, Tanaka H, Kohama K, Miki N, et al. Involvement of gicerin in the extension of microvilli. Exp Cell Res 2001; 271:269-76.
29. Guezguez B, Vigneron P, Lamerant N, Kieda C, Jaffredo T, Dunon D. Dual role of melanoma cell adhesion molecule (MCAM)/CD146 in lymphocyte endothelium interaction: MCAM/CD146 promotes rolling via microvilli induction in lymphocyte and is an endothelial adhesion receptor. J Immunol 2007; 179:6673-85.
30. Nielsen JS, Graves ML, Chelliah S, Vogl AW, Roskelley CD, McNagny KM. The CD34-related molecule Podocalyxin is a potent inducer of microvillous formation. PLoS One 2007; 2:e237.
31. Yonemura S, Nagafuchi A, Sato N, Tsukita S. Concentration of an integral membrane protein, CD43(leukosialin, sialophorin), in the cleavage furrow through the interaction of its cytoplasmic domain with actin-based cytoskeletons. J Cell Biol 1993; 120:437-49.
32. Yonemura S, Tsukita S, Tsukita S. Direct involvement of Ezrin/Radixin/Moesin (ERM)-binding membrane proteins in the organization of microvilli in collaboration with activated ERM proteins. J Cell Biol 1999; 145:1497-509.
33. Yonemura S, Hirao M, Doi Y, Takahashi N, Kondo T, Tsukita S, et al. Ezrin/radixin/moesin (ERM) proteins bind to a positively charged amino acid cluster in the juxta-membrane cytoplasmic domain of CD44, CD43 and ICAM-2. J Cell Biol 1998; 140:885-95.
34. Bretscher A. Purification of an 80,000-dalton protein that is a component of the isolated microvillus cytoskeleton, and its localization in nonmuscle cells. J Cell Biol 1983; 97:425-32.
35. Fiévet B, Louvard D, Arpin M. ERM proteins in epithelial cell organization and functions. Biochem Biophys Acta 2007; 1773:653-60.
36. Niggli V, Rossy J. Ezrin/radixin/moesin: versatile controllers of signaling molecules and of the cortical cytoskeleton. Int J Biochem Cell Biol 2008; 40:344-9.
37. Takeuchi K, Sato N, Kasahara H, Funayama N, Nagafuchi A, Yonemura S, et al. Perturbation of cell adhesion and microvilli formation by antisense oligonucleotides to ERM family members. J Cell Biol 1994; 125:1371-84.
38. Pearson MA, Reczek D, Bretscher A, Karplus PA. Structure of the ERM protein moesin reveals the FERM domain fold masked by an extended actin binding tail domain. Cell 2000; 101:259-70.
39. Hamada K, Shimizu T, Matsui T, Tsukita S, Tsukita S, Hakoshima T. Structural basis of the membrane-targeting and unmasking mechanisms of the radixin FERM domain. EMBO J 2000; 19:4449-62.
40. Li Q, Nance MR, Kulikauskas R, Nyberg K, Fehon R, Karplus PA, et al. Self-masking in an intact ERM-merlin protein: an active role for the central α-helical domain. J Mol Biol 2007; 365:1446-59.
41. Lee JH, Katakai T, Hara T, Gonda H, Sugai M, Shimizu A. Roles of p-ERM and Rho-ROCK signaling in lymphocyte polarity and uropod formation. J Cell Biol 2004; 167:327-37.
42. Kunda P, Pelling AE, Liu T, Baum B. Moesin controls cortical rigidity, cell rounding, and spindle morphogenesis during mitosis. Curr Biol 2008; 18:91-101.
43. Hao JJ, Liu Y, Kruhlak M, Debell KE, Rellahan BL, Shaw S. Phospholipase C-mediated hydrolysis of PIP2 releases ERM proteins from lymphocyte membrane. J Cell Biol 2009; 184:451-62.

44. Tsukita Sa, Oishi K, Sato N, Sagara J, Kawai A, Tsukita Sh. ERM family members as molecular linkers between the cell surface glycoprotein CD44 and actin-based cytoskeletons. J Cell Biol 1994; 126:391-401.
45. Yonemura S, Matsui T, Tsukita S, Tsukita S. Rho-dependent and -independent activation mechanisms of ezrin/radixin/moesin proteins: an essential role for polyphosphoinositides in vivo. J Cell Sci 2002; 115:2569-80.
46. Kamiguchi K, Tachibana K, Iwata S, Ohashi Y, Morimoto C. Cas-L is required for β1 integrin-mediated costimulation in human T cells. J Immunol 1999; 163:563-8.